Chinese Physics Letters

LETTER

Boundary Condition Induced Topological Transitions in Graphene Quantum Pumps: From Finite to Infinite

Cite as: Lie-Run Tian *et al*. 2026 *Chin. Phys. Lett.* **43** 090704

DOI CSTR

Recommended Articles

Floquet-Engineering Topological Phase Transition in Graphene Nanoribbons by Light
Anhua Huang, Shasha Ke, Ji-Huan Guan, Jun Li, and Wen-Kai Lou
Chin. Phys. Lett. **41**, (2024)

Bound States in the Continuum of Infinite Quality Factor in Finite Unit Cells
Hua-Wei Liang, Yuan-Zhi Liu, Yu-Jia Zeng, Yang-Jian Cai, and Ting-Yin Ning
Chin. Phys. Lett. **42**, 080401 (2025)

Symmetry Breaking and Phase Transitions in Twisted Rhombohedral Trilayer-Bilayer Graphene
Jingwei Dong *et al*.
Chin. Phys. Lett. **43**, 060716 (2026)

Manipulation of Topological Boundaries within a Magnetic Domain Wall
Zhuyang Nie, Ji Chen, Cunlong Dong, Bin He, Caihua Wan, Haifeng Du, Xiufeng Han, Yizhou Liu, and Guoqiang Yu
Chin. Phys. Lett. **43**, 050715 (2026)

Localized Topological States in Finite Non-Hermitian Photonic Lattices
Xiong Fan, Wenchi Zang, Ming Ma, Li-Gang Wang, and Tianxing Ma
Chin. Phys. Lett. **43**, 040701 (2026)

A series journal of Chinese Physical Society distributed by IOP Publishing

Chinese Physics Letters

Chin. Phys. Lett. **43** 090704 (2026)

LETTER

DOI: 10.1088/0256-307X/43/9/090704
CSTR: 32039.14.0256-307X.43.9.090704

Boundary Condition Induced Topological Transitions in Graphene Quantum Pumps: From Finite to Infinite

Lie-Run Tian[1,2,3,†], Hao-Kun Ke[1,†], Xuan-Feng Liang[2,3], Jin-Zhu Zhao[2,3,4], Jun-Feng Liu[1,*], and Jun Wang[5,*]

[1]School of Physics and Materials Science, Guangzhou University, Guangzhou 510006, China
[2]Guangdong Basic Research Center of Excellence for Structure and Fundamental Interactions of Matter, Guangdong Provincial Key Laboratory of Quantum Engineering and Quantum Materials, School of Physics, South China Normal University, Guangzhou 510006, China
[3]Guangdong-Hong Kong Joint Laboratory of Quantum Matter, Frontier Research Institute for Physics, South China Normal University, Guangzhou 510006, China
[4]Center for Computational Science and Engineering, Southern University of Science and Technology, Shenzhen 518055, China
[5]Department of Physics, Southeast University, Nanjing 210096, China

[†]These authors contributed equally to this work.
[*]Corresponding authors. Email: phjfliu@gzhu.edu.cn; jwang@seu.edu.cn

We investigate the quantized charge pumping in graphene with Rashba spin–orbit coupling (RSOC) under two time-periodic staggered potentials. Surprisingly, the quantized charge pumped per cycle exhibits a sharp dependence on the transverse boundary conditions: a zero quantized charge is obtained under periodic boundary conditions (consistent with bulk thermodynamic limits), whereas a quantized value of 1 per spin emerges under open boundary conditions. This topological transition induced by the transverse boundary conditions persists even for large system widths, revealing a discontinuous crossover from finite to infinite geometries without relying on topological edge states at the boundaries. We attribute this phenomenon to RSOC-induced intravalley reflection at transverse boundaries, which modifies the winding number of the pumping cycle. These results challenge conventional wisdom about finite-to-infinite transitions in condensed matter systems and advance the fundamental understanding of boundary-sensitive quantum transport in multivalley systems.

Introduction

In condensed matter physics, the transition from finite to infinite system size is conventionally regarded as a smooth process [1−5]. Finite systems with boundaries are described by open boundary conditions (OBCs), whereas infinite systems without boundary correspond to periodic boundary conditions (PBCs). At sufficiently large scales, boundary effects are generally assumed to negligibly influence bulk properties [6−11]. The established exception occurs in topologically nontrivial systems hosting topological edge states (TESs) which heavily change the property of the system even at sufficiently large scales [12−22]. For example, the conductance of a quantum anomalous Hall insulator (QAH) ribbon with a chiral edge state is always one conductance quantum no matter how large the ribbon width is. However, the conductance of an infinite QAH system or a QAH ribbon with PBCs is zero if only the Fermi energy is beside the topological gap. Yet, when TESs are absent, whether non-TESs mechanisms could drive abrupt transitions between finite and infinite limits remains an unresolved fundamental question [23−29]. This challenges the conventional wisdom that boundary effects can be neglected in large-scale systems.

On the other hand, topological transitions, typically driven by external fields (e.g., electric or magnetic fields) or interactions, are paradigmatic examples of discontinuous changes in quantum systems [30−34]. Boundary-relevant topological transitions by light, strain, or doping in multivalley systems such as graphene nanoribbons have also been reported [35−38]. While boundary conditions are known to modify local electronic properties, their role in triggering global topological transitions has been widely assumed negligible due to the perceived continuity of boundary effects [39−41]. This assumption persists despite growing evidence of spin–orbit coupling (SOC) reshaping quantum transport near edges or interfaces.

Here, we reveal a boundary-condition-driven topological transition that defies conventional wisdom. By analyzing topological pumps based on graphene with Rashba SOC (RSOC), we demonstrate that PBCs—a cornerstone of bulk-property approximations—fail when intravalley reflection occurs at transverse edges. This reflection modifies the quantization condition of the transverse wave vector required by PBCs and generates a discontinuous jump in pumped charge (from 0 to 1 per cycle) as the system transitions from PBCs to OBCs. Crucially, this mechanism operates without TESs, establishing a new paradigm for finite-to-infinite crossover physics. Our work redefines the applicability criteria of PBCs in multivalley systems and exposes a hidden interplay between spin-valley hybridization and quantum transport.

Model and Methods

As illustrated in Fig. 1, we investigate a two-parameter pump based on monolayer graphene with RSOC. RSOC is considered within the device region but absent in the leads. Two time-dependent staggered potentials, Δ_1 and Δ_2, are applied in two regions with a length L to open a gap. At the transverse boundaries, the upper and lower edges are connected by dashed lines with a tunable hopping energy $t_B \in [0, t_0]$, where $t_B = 0$ corresponds to the OBC and $t_B = t_0$ recovers the PBC. This setup enables a continuous interpolation between finite and infinite systems. Notably, the transport and the transverse boundaries are chosen to be along the armchair direction to exclude the influence of zigzag edge states. The lattice Hamiltonian of this pump is given as follows:

$$H = H_0 + H_R + V(t), \tag{1}$$

where

$$H_0 = -t_0 \sum_{\langle i,j \rangle} c_i^\dagger c_j, \tag{2}$$

Received 2 May 2026; accepted 17 August 2026; published 7 September 2026
© 2026 Chinese Physical Society and IOP Publishing Ltd. All rights, including for text and data mining, AI training, and similar technologies, are reserved.

Check for updates

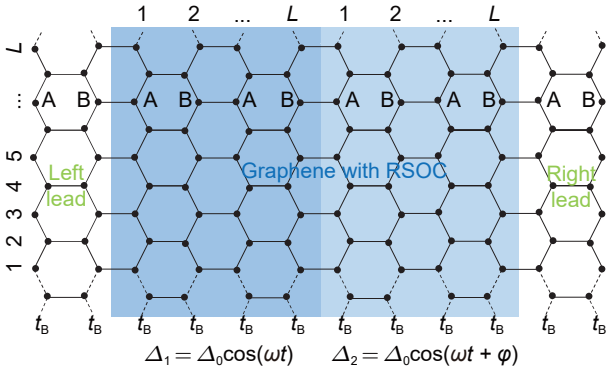

Fig. 1. The sketch of a two-parameter pump based on monolayer graphene with RSOC. The pump is driven by two time-dependent staggered potentials, Δ_1 and Δ_2, which are applied in two regions with the same length L. RSOC is present throughout the device region but absent in two leads. At the transverse boundaries, the upper and lower edges are connected by dashed lines with a tunable hopping energy $t_B \in [0, t_0]$, where $t_B = 0$ corresponds to the OBC and $t_B = t_0$ recovers the PBC

$$H_R = -i\frac{t_R}{a}\sum_{\langle i,j\rangle} c_i^\dagger \hat{e}_z \cdot (\boldsymbol{s}\times \boldsymbol{d}_{ij})\, c_j, \tag{3}$$

$$V(t) = \sum_i \mu_i[\Delta_1(x,t) + \Delta_2(x,t)]c_i^\dagger c_i, \tag{4}$$

with

$$\Delta_1(x,t) = \Delta_1(t)[\Theta(x) - \Theta(x-L)],$$
$$\Delta_2(x,t) = \Delta_2(t)[\Theta(x-L) - \Theta(x-2L)].$$

Here, H_0 denotes the Hamiltonian of pristine graphene, $c_i^\dagger$ (c_i) are the creation (annihilation) operator for electrons at site i, and t_0 is the hopping energy between the nearest-neighbor sites. H_R represents the RSOC term, with t_R the RSOC strength and a the c-c bond length. $\boldsymbol{d}_{ij}$ is the lattice vector pointing from site j to site i, and $\boldsymbol{s}$ is the vector of Pauli matrices in spin space. The time-dependent potential $V(t)$ consists of two components, Δ_1 and Δ_2, which are applied in two regions $[0, L]$ and $[L, 2L]$, respectively. $\mu_i = +(-)1$ for the ith site representing the carbon A(B) atom. The staggered potentials $\Delta_1 = \Delta_0\cos(\omega t)$ and $\Delta_2 = \Delta_0\cos(\omega t + \varphi)$ are uniformly applied in two regions with length L as shown in Fig. 1. There, ω is the pumping frequency, Δ_0 is the pumping strength, and φ is the pumping phase shift.

The staggered potentials Δ_1 and Δ_2 break the inversion symmetry in graphene [42,43], and open an energy gap at the Dirac points. When two staggered potentials Δ_1 and Δ_2 have opposite signs, topological interface states (TISs) emerge between the two regions [44]. It has been demonstrated that a quantized charge is pumped in a cycle [$\Delta_1(t)$ and $\Delta_2(t)$ undergoing a cycle of evolution] just due to the adiabatic evolution of these TISs [45].

In the adiabatic limit $\omega \to 0$, the pumped current is calculated using the the Büttiker-Pretre-Thomas (BPT) formalism [46]

$$I_\alpha = \frac{ie}{2\pi T}\int_0^T dt \left(\frac{\partial S_t}{\partial t} S_t^*\right)_{\alpha\alpha}. \tag{5}$$

Here, $\alpha = L(R)$ represents the left (right) lead, e is the electron charge, $T = 2\pi/w$ is the pump period. S_t is the instantaneous scattering matrix, which is obtained by the Fisher-Lee formula [47]

$$S_{t\alpha\beta} = -\delta_{\alpha\beta} + i(\Gamma_\alpha)^{1/2} G_t^r (\Gamma_\beta)^{1/2}. \tag{6}$$

For numerical convenience, we use the Green's function method to rewrite Eq. (5) as [48]

$$I_\alpha = \frac{e}{2\pi T}\oint dt\, \mathrm{Tr}\left[\Gamma G_t^r \dot{V} G_t^a\right]_{\alpha\alpha}. \tag{7}$$

The line-width matrix of the leads is defined as $\Gamma_\alpha = i\left[\Sigma_\alpha^r - (\Sigma_\alpha^r)^\dagger\right]$, where Σ_α^r represents the self-energy of the leads and can be calculated through the surface Green's function and by the recursive Green's function method. The instantaneous retarded Green's function of the scattering region is $G_t^r = \left[EI - H(t) - \Sigma_L^r - \Sigma_R^r\right]^{-1}$, and the advanced Green's function is given by $G_t^a = (G_t^r)^\dagger$. Here $H(t)$ denotes the instantaneous Hamiltonian of the scattering region. $\dot{V}$ is the time derivative of the pumping potential.

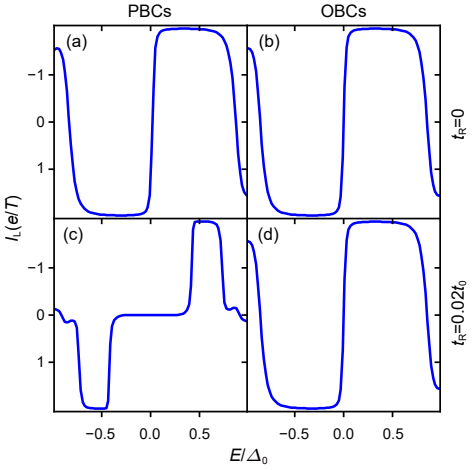

Fig. 2. The pumped current I_L as a function of Fermi energy E under OBCs ($t_B = 0$) and PBCs ($t_B = t_0$), without ($t_R = 0$) and with ($t_R = 0.02t_0$) RSOC. The parameters are taken as $\Delta_0 = 0.03t_0$, $\varphi = \pi/2$, $L = 50$, $N = 23$.

Boundary Condition Induced Topological Transition

We numerically calculate the pumped current I_L in a monolayer graphene nanoribbon with width $N = 23$ and length $L = 50$, as shown in Fig. 1. The pumped current is plotted in Fig. 2 as a function of Fermi energy E under OBCs and PBCs, respectively. We systematically compare the regimes with and without RSOC. At low energies, the pumped current is quantized to 2 (1 per spin) or 0 due to the topologically nontrivial nature of the pump. Under PBCs, the pump undergoes a topological transition in the energy window $[-0.4\Delta_0, 0.4\Delta_0]$ when RSOC is turned on [49]. The pumped current changes from ± 2 to 0 for positive or negative energies. Under OBCs, this topological transition of the pump vanishes. From an alternative perspective, when RSOC vanishes, both PBCs and OPCs yield identical quantized pumping currents. Conversely, finite RSOC induces a discontinuity, resulting in divergent pumping behaviors under PBCs versus OBCs. Our numerical results reveal that this boundary condition induced topological transition persists even for substantially large widths, suggesting that the finite-to-infinite crossover is a discontinuous topological transition.

To investigate the continuous crossover from OBCs to PBCs, we define the boundary hopping energy t_B which connects the upper and lower boundaries as shown in Fig. 1. The change of t_B from 0 to t_0 enables a continuous interpolation between OBCs and PBCs. Figure 3 plots the pumped current as a function t_B for various Fermi energies E. When $E \in [0, 0.4\Delta_0]$, the current undergoes a discontinuous topological transition from the quantized value 2 to 0 at a critical value t_B^c. The critical boundary hopping energy t_B^c increases with increasing Fermi energy E.

When the Fermi energy E resides within the gap opened by two staggered potentials, incident electrons are completely reflected during the full pumping period T. Therefore, the transmission matrix is always zero during the pumping cycle. The topological phase and topological transition can be directly characterized by the winding number of the pump from the reflection matrix $\mathcal{R}$ as follows [50]:

$$W = \frac{1}{2\pi i}\oint d\{\ln[\det(\mathcal{R})]\}, \tag{8}$$

where $\det(\mathcal{R})$ represents the determinant of the reflection amplitude

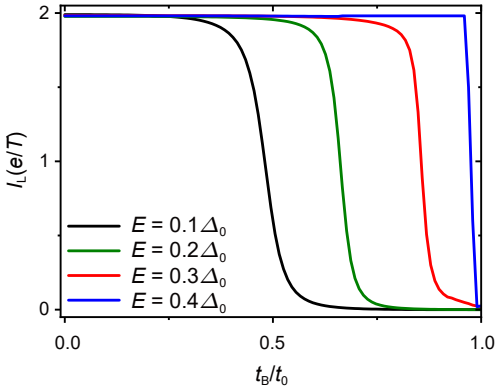

Fig. 3. The pumped current I_L as a function of tunable hopping amplitude t_B for various Fermi energy E. The parameters are taken as $\Delta_0 = 0.03t_0$, $\varphi = \pi/2$, $L = 50$, $N = 23$, $t_R = 0.02t_0$.

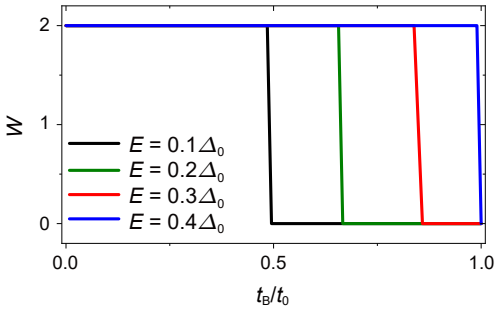

Fig. 4. The Winding number W as a function of tunable hopping amplitude t_B for various Fermi energy E. The parameters are taken as $\Delta_0 = 0.03t_0$, $\varphi = \pi/2$, $L = 50$, $N = 23$, $t_R = 0.02t_0$.

matrix $\mathcal{R}$ which is obtained by Eq. (6) when α and β denote the same lead.

In Fig. 4, we present the evolution of the winding number W of the pump as a function of the boundary hopping energy t_B. Our results demonstrate that the winding number is $W = 2$ under OBCs, but becomes $W = 0$ under PBCs. The former case corresponds to a quantized pumped charge of 2 per cycle, whereas the latter yields no net charge transport. This behavior of W is consistent with that of the pumping current. By identifying the winding number W as a topological invariant, we thus confirm the occurrence of a topological transition in the pumping process. The topology of the quantized pump can also be characterized by the shift of the electron Wannier function's centers in the lattice, as shown in Section S1 of the Supplemental Material (SM).

From Finite to Infinite

It is found that the band structure of armchair graphene ribbons (AGRs) is the same for $t_b = 0$ and $t_b = t_0$ when $t_R = 0$ due to the completely intervalley reflection at the boundaries (see Section S2 of the SM). Therefore, there is no boundary condition induced topological transition when RSOC is absent. When RSOC is present, in the low-energy limit, the intervalley reflection is prohibited and only the intravalley reflection is allowed at boundaries. The band structures of AGNs are distinctly different under OBCs versus PBCs. Although the difference diminishes with increasing width, the eigenstates remain persistently distinct. This persistent wavefunction disparity constitutes the root physical origin of the boundary condition induced topological transition. Therefore, this topological transition persists even for substantially large widths. Due to limited computing capabilities, we calculate the pumped current in a ribbon with a width up to $N = 2000$, still showing the persistence of this transition.

In infinite systems, we consider the transverse wave vector as a good quantum number finally integrate over the wave vector. This is consistent with the PBCs if only the width is substantially large. Usually we assume that a system can be dealt with as an infinite system if the scale is sufficiently large. The boundary condition induced topological transition overturns this established dogma. This finite-to-infinite topological transition demonstrates that the continuous crossover between finite and infinite systems may be nonexistent.

Besides, we briefly comment on the situation of zigzag graphene ribbons (ZGRs). Under PBCs, the pumped current in ZGRs is the same as that in AGRs. However, under OBCs, due to the presence of zigzag edge states, the pumped current is not quantized. Therefore, the boundary condition induced topological transition can not be observed in ZGRs (see Section S3 of the SM).

Finally, we comment on the experimental feasibility of this boundary condition induced topological transition. By proximity coupling graphene to Ni substrates, the RSOC strength can reach up to 100 meV [51]. The time-dependent staggered potentials can be engineered using hexagonal boron nitride substrates [52]. A dual-gate can be utilized to produce a vertical electric field to tune the magnitude of the staggered potentials. We will study the quantum pump based on the bilayer and trilayer graphene with RSOC in our future works and investigate the PBC-OBC transition, where the time-periodic staggered potentials will be more experimentally feasible via a vertical electric field.

Conclusion

In summary, our work establishes a paradigm-shifting mechanism for boundary-condition-driven topological transitions beyond the conventional knowledge on the boundary effect. Through graphene-based quantum pumps with RSOC, we demonstrate that transverse boundary conditions alone can induce a discontinuous jump in quantized charge pumping (from 0 to 1 per spin per cycle), despite the absence of TESs. Crucially, this transition persists at large widths, defying the expectation that boundary effects vanish in large systems. The key enabler is RSOC-activated intravalley reflection, which disrupts PBC quantization of the transverse wave vector at open boundaries. This mechanism advances the fundamental understanding of boundary-sensitive quantum transport in multivalley systems and enables tunable topological transition via boundary engineering. These findings reshape our fundamental understanding of finite-to-infinite crossovers and open pathways for boundary-controlled topological electronics.

Acknowledgements

This work was supported by the National Natural Science Foundation of China (Grant Nos. 12174077, 12174051, and 12274145) and the Bureau of Education of Guangzhou Municipality (Grant No. 202255464).

References

[1] Phien H N, Vidal G, and McCulloch I P 2009 *Phys. Rev. B* **86** 245107
[2] Landau D P 1976 *Phys. Rev. B* **13** 2997
[3] Zhu X, Wang H X, Xu C, Lai Y, Jiang J H, and John S 2018 *Phys. Rev. B* **97** 085148
[4] Corboz P, Czarnik P, Kapteijns G, and Tagliacozzo L 2018 *Phys. Rev. X* **8** 031031
[5] Ebisu H and Watanabe M 2021 *Phys. Rev. B* **104** 195124
[6] Watanabe H 2018 *Phys. Rev. B* **98** 155137
[7] Wang S S, Yu Y, Guan J H, Dai Y M, Wang H H, and Zhang Y Y 2022 *Phys. Rev. B* **106** 075136
[8] Zhang Z Q, Liu H, Liu H, Jiang H, and Xie X C 2023 *Sci. Bull.* **68** 157
[9] Lebowitz J L and Lieb E H 1969 *Phys. Rev. Lett.* **22** 631
[10] Brout R 1960 *Phys. Rev.* **118** 1009
[11] Kohn W and Sham L J 1965 *Phys. Rev.* **140** A1133
[12] Kane C L and Mele E J 2005 *Phys. Rev. Lett.* **95** 226801
[13] Bernevig B A and Zhang S C 2006 *Phys. Rev. Lett.* **96** 106802
[14] Haldane F D M 1988 *Phys. Rev. Lett.* **61** 2015

[15] König M, Wiedmann S, Brüne C, Roth A, Buhmann H, Molenkamp L W, Qi X L, and Zhang S C 2007 *Science* **318** 766
[16] Hasan M Z and Kane C L 2010 *Rev. Mod. Phys.* **82** 3045
[17] Qi X L and Zhang S C 2011 *Rev. Mod. Phys.* **83** 1057
[18] Moore J E and Balents L 2007 *Phys. Rev. B* **75** 121306
[19] Fu L and Kane C L 2008 *Phys. Rev. Lett.* **100** 096407
[20] Ma G, Xiao M, and Chan C T 2019 *Nat. Rev. Phys.* **1** 281
[21] Lu L, Joannopoulos J D, and Soljacic M 2014 *Nat. Photon.* **8** 821
[22] Zhou D, Rocklin D Z, Leamy M, and Yao Y 2022 *Nat. Commun.* **13** 3379
[23] Kurzyna M and Kwapiński T 2020 *Phys. Rev. B* **102** 195429
[24] Lin Q, Li T, Xiao L, Wang K, Yi W, and Xue P 2022 *Nat. Commun.* **13** 3229
[25] Sone K, Ezawa M, Gong Z, Sawada T, Yoshioka N, and Sagawa T 2025 *Nat. Commun.* **16** 422
[26] Jang Y, Kim S, Kim M, Kim G, Kim E, and Rho J 2025 *Extreme. Mech. Lett.* **77** 102334
[27] Fu Y, Huang Y, and He Q L 2025 *Nat. Commun.* **16** 3058
[28] Zhang X, Zangeneh-Nejad F, Chen Z G, Lu M H, and Christensen J 2023 *Nature* **618** 687
[29] Gao N, Wen Z, Yang M, Jiang W, Wu B, Qu Y, Romero-García V, Bao R, Wang J, and Chen W 2025 *Small Struct.* **6** 2500319
[30] Huang Z M and Diehl S 2025 *Phys. Rev. Lett.* **134** 053002
[31] Yang N J, Zhang J M, Li X P, Zhang Z, Yu Z M, Huang Z, and Yao Y 2025 *Phys. Rev. Lett.* **134** 256602
[32] Tong P, Zhou L, Du K *et al*. 2025 *Nat. Phys.* **21** 464
[33] Zhong J, Yang M, Zhao W *et al*. 2025 *Nat. Commun.* **16** 1163
[34] He C, Zhao L, Zhang S, Zhou L, and Ma S 2025 *eLight* **5** 19
[35] Huang A, Ke S, Guan J H, Li J, and Lou W K 2024 *Chin. Phys. Lett.* **41** 097302
[36] Huang A, Ke S, Guan J H, Li J, and Lou W K 2024 *Phys. Rev. B* **109** 045408
[37] Wang W, Lv X, and Xie H 2021 *Chin. Phys. B* **30** 066701
[38] Gao Y, Zeng X, and Zhang R 2026 *Chin. Phys. B* **35** 037103
[39] Zhang G, Cao Z, and Liu D E 2024 *Phys. Rev. B* **109** L161110
[40] Xu G, Li Y, Li W, Fan S, and Qiu C W 2021 *Phys. Rev. Lett.* **127** 105901
[41] Li L H and Chen S 2015 *Phys. Rev. B* **92** 085118
[42] Xiao D, Yao W, and Niu Q 2007 *Phys. Rev. Lett.* **99** 236809
[43] Wang S K, Wang J, and Chan K S 2014 *New J. Phys.* **16** 045015
[44] Ezawa M 2013 *Phys. Rev. B* **88** 161406
[45] Ding Z, Wang S, Li M, Tao Y, and Wang J 2023 *New J. Phys.* **25** 123039
[46] Büttiker M, Prêtre A, and Thomas H 1994 *Z. Phys. B: Condens. Matter* **94** 133
[47] Fisher D S and Lee P A 1981 *Phys. Rev. B* **23** 6851
[48] Wang X H, Wang J J, Wang J, and Liu J F 2021 *Phys. Rev. B* **103** 195442
[49] Tian L R, Tan H, Liu J F, Wang J, and Zhao J Z 2025 *Phys. Rev. B* **111** 195422
[50] Avron J E, Elgart A, Graf G M, and Sadun L 2004 *J. Stat. Phys.* **116** 425
[51] Cheng X, Xiao L, and Zhai X 2024 *Phys. Rev. B* **109** 035426
[52] Wong S S, Lin Z Y, Ho S Z *et al*. 2025 *Adv. Mater.* **37** 2414442